iScience

CellPress
OPEN ACCESS

Article

Mycobacterial SapM hampers host autophagy initiation for intracellular bacillary survival via dephosphorylating Raptor

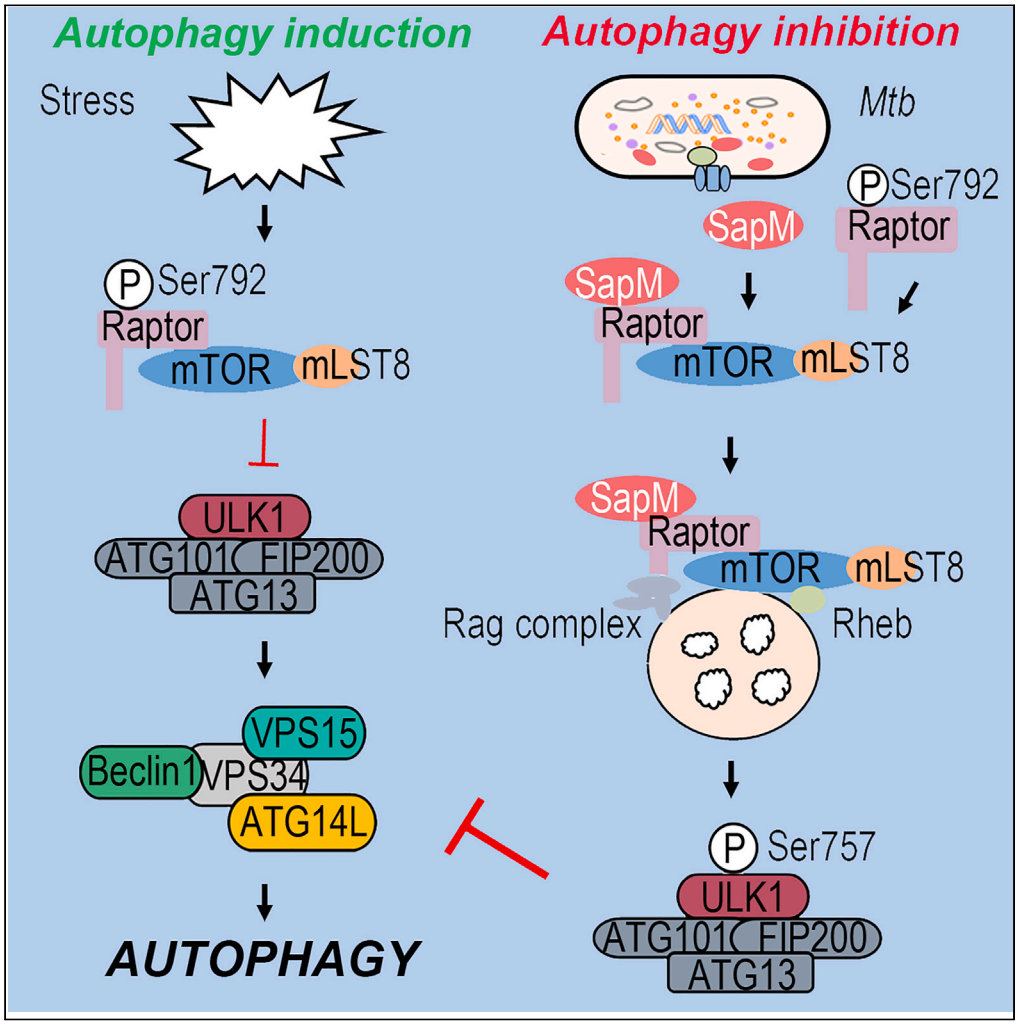

Wei Zhang, Chunsheng Dong, Sidong Xiong

chunshengdong@suda.edu.cn (C.D.)
sdxiong@suda.edu.cn (S.X.)

Highlights

SapM hampers autophagy induction

SapM impedes autophagy induction by enhancing mTORC1 activity

SapM increases the mTORC1 activity via dephosphorylating Raptor

SapM alleviates the lung pathological progression in the infected mice

Zhang et al., iScience *27*, 109671
May 17, 2024
https://doi.org/10.1016/j.isci.2024.109671

iScience

CellPress
OPEN ACCESS

Article

Mycobacterial SapM hampers host autophagy initiation for intracellular bacillary survival via dephosphorylating Raptor

Wei Zhang,[1] Chunsheng Dong,[1,2,*] and Sidong Xiong[1,3,*]

SUMMARY

Secreted acid phosphatase (SapM) is an immunomodulator of *Mycobacterium tuberculosis (Mtb)* and consequently plays a crucial role in disease onset and development upon infection. Importantly, the virulence of SapM has rendered SapM an attractive target for drug development. However, the mechanism underlying the role of SapM in facilitating bacillary survival remains to be fully elucidated. In this context, the present study demonstrated that SapM hampered cellular autophagy to facilitate bacillary survival in *mycobacterial*-infected macrophages. Mechanically, SapM interacted with Raptor and was localized to the subcellular lysosomal organelle, causing the dephosphorylation of Raptor at the Ser792 position, resulting in mTORC1 hyperactivity and the subsequent autophagy inhibition. Consistent with this, SapM blocked the autophagy initiation and mitigated lung pathology *in vivo*. These findings highlighted the role of Raptor as a significant substrate of SapM for inhibiting autophagy, which is a novel clue for developing a treatment against tuberculosis.

INTRODUCTION

Tuberculosis (TB) is a disease that occurs upon infection with *Mtb*. TB continues to be a major threat to global public health, particularly in low-income and middle-income nations. In 2022, over $13 billion was spent on TB prevention, diagnosis, treatment, and care across the globe.[1] Among the individuals affected with *Mtb*, only 10% develop active TB, while the remaining 90% develop latent TB in which the microbe persists within the individual for years or even decades. Traditional antibiotics such as isoniazid, rifampicin, pyrazinamide, streptomycin, and ethambutol are used as the first-line anti-TB drugs, although the efficacy of these drugs is limited due to drug resistance. Bedaquiline is a novel small-molecule drug, which has recently been reported as a promising drug in the treatment of drug-resistant TB, although safety concerns regarding its use remain to be addressed.[2] Therefore, it is imperative to develop innovative therapeutic strategies for TB treatment.

Host-directed therapy (HDT) is a novel adjuvant therapy for TB, which involves using pharmacological means to target host effectors to enhance the immune response against *Mtb*. Multiple host cell processes, including phagocytosis, autophagy, apoptosis, necrosis, and ferroptosis, have been identified as potential targets for HDT.[3,4] Among these processes, autophagy is considered the most promising target for HDT, particularly owing to its role in limiting the survival of *Mtb*, in addition to its function of maintaining cellular integrity and homeostasis in host cells.[5–8] Autophagy is a highly conserved process that involves the degradation of cytoplasmic components, including the damaged or redundant organelles and toxic protein aggregates in eukaryotic cells. Macroautophagy (hereafter referred to as "autophagy") is the major type of autophagy, which has been investigated the most among all types of autophagy.[9] It comprises four stages including induction of autophagy initiation, formation of autophagosome, the fusion of the autophagosome with the lysosome, and degradation of the engulfed contents.[10]

Autophagy may be induced by various stress signals, such as starvation, hypoxia, and microbial infection.[11,12] Typically, ULK1 is reported as a significant initiator of autophagy. Upon autophagy induction, the ULK1 complex comprising ULK1, FIP200, ATG13, and ATG101 translocates to the autophagy initiation sites to regulate the recruitment of another kinase complex referred to as the VPS34 complex. This VPS34 complex comprises VPS34, Beclin-1, VPS15, and ATG14L and generates phospholipid phosphatidylinositol 3-phosphate (PI3P) at the site of formation of the autophagosome, referred to as a phagophore. The produced PI3P then binds with PI3P-binding proteins such as WIPI2B and DFCP1, which are also recruited at the site. This binding, together with other proteins, leads to the formation and expansion of the phagophore, which is eventually sealed, forming the complete autophagosome.[13]

The mTORC1 complex is the master regulator of the cell's response to nutrient availability in the early stage of autophagy induction.[14] This complex is approximately 1 MDa in size and comprises mTOR, Raptor, mLST8, PRAS40, and DEPTOR as its main components. Under

[1]Jiangsu Key Laboratory of Infection and Immunity, Institutes of Biology and Medical Sciences, Suzhou Medical College of Soochow University, Suzhou 215123, China
[2]Key Laboratory of Geriatric Diseases and Immunology, Ministry of Education, Institutes of Biology and Medical Sciences, Suzhou Medical College of Soochow University, Suzhou 215123, China
[3]Lead contact
*Correspondence: chunshengdong@suda.edu.cn (C.D.), sdxiong@suda.edu.cn (S.X.)
https://doi.org/10.1016/j.isci.2024.109671

adequate nutrient levels, the activity of the mTORC1 complex is high, which prevents ULK1 activation through the phosphorylation of the Ser757 residue in ULK1, thereby disrupting the interaction between ULK1 and AMPK.[15] In the amino acid deprivation scenario, mTORC1 activation on the lysosomal surface does not occur, and both ULK1 and ATG13 are rapidly dephosphorylated, which results in the activation of ULK1 kinase and the concomitant autophagy induction. The activation of mTORC1 includes the translocation of mTORC1 onto the lysosomal surface for amino acid-dependent signaling. The addition of amino acids induces the transformation of Rag GTPases into their active nucleotide-bound state, i.e., the heterodimer comprising the GTP-bound form of RagA/B and the GDP-bound form of RagC/D. Active Rag GTPases bind to Raptor to recruit mTORC1 onto the lysosomal surface, where Rheb, a direct activator of mTORC1, is also located. In contrast, greater amounts of mTORC1 are released into the cytosol in the presence of inactive GTPases and Rheb, leading to the inhibition of mTORC1 activity.[16] Moreover, AMPK was recently reported to phosphorylate Raptor on a highly conserved serine residue, thereby inhibiting the mTORC1 activity.[17,18]

Rv3310 is a secreted acid phosphatase (SapM) encoded by *Mtb*. In 2020, Pisu and colleagues performed a dual RNA-seq on ontogenetically distinct macrophage lineages isolated from *Mycobacterium*-infected murine lungs to explore the *in vivo* molecular dynamics of *Mtb* infection in alveolar macrophages that are supposed to sustain *Mtb* growth and also in interstitial macrophages that restrict *Mtb* growth.[19] Interestingly, based on their RNA-seq data, the present study revealed SapM as one of the differentially expressed genes (with its expression 2-fold higher in the alveolar macrophages compared to that in the interstitial macrophages). A previous study had also indicated that SapM potently promoted bacterial survival in mice and Guinea pigs.[20] However, the mechanism underlying the role of SapM in facilitating bacillary survival remains to be elucidated to date. In this context, the present study revealed that SapM interacted with Raptor and dephosphorylated the Ser792 residue in Raptor, leading to mTORC1 hyperactivity, thereby inhibiting autophagy induction, and facilitating intracellular bacillary survival. Overall, the findings of the present study demonstrated the potential of mTORC1 in regulating autophagy signaling to facilitate HDT strategies against *Mtb* infection.

RESULTS

Mycobacterial SapM facilitated bacillary survival *in vitro* and *in vivo*

SapM is not present in *M. smegmatis (Ms)*. In order to investigate the function of SapM, a recombinant *Ms* that exogenously expresses the *Mtb* SapM (*Ms::SapM*) was constructed along with its control strain *Ms::WT*(Figure S1A). Although the bacillary growth in the culture medium was similar for *Ms::SapM* and *Ms::WT* (data not presented), the bacillary loads in the *Ms::SapM*-infected RAW264.7 cells (Figure 1A) and THP-1 cells (Figure 1B) were higher than the bacillary load in the control group after 48 h of infection which suggested that SapM promoted *Ms* survival in the infected macrophages. In order to further investigate the function of SapM in bacillary survival in the *Mtb*-infected macrophages, an *H37Rv*-knockout SapM strain (*H37RvΔSapM*) was constructed along with its rescue strain (*H37RvΔSapM::SapM*)(Figure S1B). It was observed that the bacillary loads were decreased by 1.5-folds in the *H37RvΔSapM*-infected RAW264.7 cells compared to the *H37Rv*-infected cells and the *MtbΔSapM::SapM*-infected cells 8 h post-infection (Figure 1C). This further demonstrated that SapM promoted *mycobacterial* survival in the infected cells. Similar results were obtained for the human leukemia monocyte (THP-1) cells (Figure 1D). In order to validate whether the exogenous SapM expression in cells affected *mycobacterial* survival, the RAW264.7 cells with a stable expression of SapM (RAW_SapM) were established (Figure S1C). These RAW_SapM cells were then infected with *Ms* or *H37Rv* for different durations. Consistent with the above results, the exogenous expression of SapM in RAW264.7 cells was observed to significantly increase *Ms*, *H37Rv* (Figures 1E and 1F), and SapM-deficient *H37Rv* cell survival (Figure 1G). In order to further investigate whether SapM potentiated *mycobacterial* survival *in vivo*, the *Ms*-infected mouse model was established. On Day 6 post-infection, it was observed that the bacillary loads were significantly increased in the lung tissues of *Ms::SapM*-infected mice compared to those of the control group mice (Figure 1H). Similarly, when the mice were infected with *Ms::mCherry-WT* and *Ms::mCherry-SapM*, higher mCherry fluorescence was observed in the lung tissues of *Ms::mCherry-SapM*-infected mice (Figure 1I). These results demonstrated that SapM indeed facilitated *mycobacterial* survival both *in vitro* and *in vivo*.

SapM hampered autophagy induction

Autophagy is utilized as an effective defense strategy by the host cell to clear *Mtb*.[21] Several *mycobacterial* virulent factors, such as PknG, Eis, and Rv0790c, reportedly modulate cellular autophagy to facilitate the escape of *Mtb* from host cell immune surveillance.[22–24] In order to determine whether SapM affected cellular autophagy, RAW264.7 cells were infected with *Ms::SapM* or the control *Ms::WT*, followed by the determination of the degree of autophagy using multiple assays. The results of flow cytometry (Figures 2A and 2B), transmission electron microscopy (Figure 2C), and western blotting (Figures 2D–2F) indicated that the *Ms::SapM*-infected RAW264.7 cells exhibited a lesser degree of autophagy compared to the *Ms::WT*-infected cells. Similar results were detected in the bone marrow-derived macrophage (BMDM),THP-1, and human monocyte-derived macrophage (hMDM) cells (Figure S2). In addition, compared to the control group, the *H37RvΔSapM*-infected macrophages exhibited dramatically increased levels of the endogenous LC3II protein and potently decreased p62 protein level. However, the LC3II protein decreased and p62 increased after complementing with SapM (Figures 2G–2I). In order to validate whether the exogenous SapM expression in macrophages affected autophagy induction, RAW_SapM cells were established and subjected to the determination of LC3 levels upon Rapamycin treatment. The cellular expression of SapM was observed to potently inhibit the LC3 levels compared to the control group, at the time points of 2 h and 4 h after the Rapamycin stimulation (Figures 2J and 2K). This result suggested that SapM suppressed autophagy induction even without the bacterial infection.

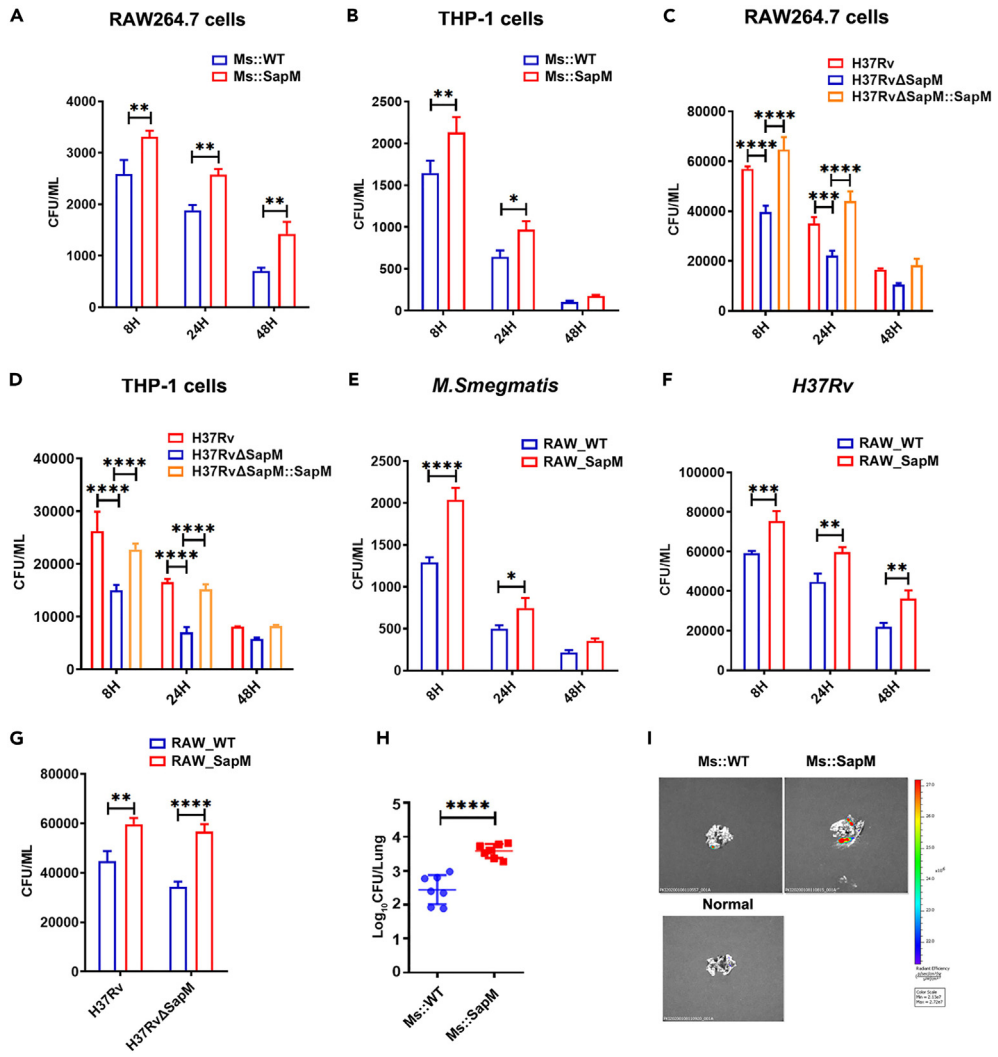

Figure 1. SapM facilitated *mycobacteria* survival both *in vitro* and *in vivo*

(A and B) RAW264.7 cells or THP-1 cells were infected with *Ms::WT* or *Ms::SapM* (MOI = 10), and the intracellular bacillary loads were detected using the CFU assay.

(C and D) RAW264.7 cells or THP-1 cells were infected with *H37Rv*, *H37RvΔSapM*, or *H37RvΔSapM::SapM* (MOI = 10), and the intracellular bacillary loads were detected using the CFU assay.

(E and F) RAW_WT cells and RAW_SapM cells were infected with *Ms* or *H37Rv* (MOI = 10), and the intracellular bacillary loads were detected using the CFU assay.

(G) RAW_WT cells and RAW_SapM cells were infected with *H37Rv* and *H37RvΔSapM*, and the intracellular bacillary loads were detected using the CFU assay.

(H) C57BL/6 mice were intranasally infected with *Ms::WT* and *Ms::SapM* for 6 days, followed by an evaluation of the intracellular bacillary loads using the CFU assay.

(I) C57BL/6 mice were intranasally infected with *Ms::mcherry-WT* and *Ms::mcherry-SapM* for 6 days, followed by measuring the fluorescence intensity using small-animal imaging. *$p < 0.05$; **$p < 0.01$; ***$p < 0.001$; ****$p < 0.0001$. Statistical analyses were performed in (C and D) using one-way ANOVA and in (A, B, E, F, G, and H) using t test. The data presented are mean ± SD and representative of a minimum of three independent experiments.

In order to further precisely determine the stage of autophagy affected by SapM, it was investigated whether SapM regulated the key molecules of autophagy induction. It was observed that compared to the control group (*Ms::WT*-infected macrophages), the *Ms::SapM*-infected macrophages exhibited significantly decreased Beclin-1 levels and increased levels of phosphorylated ULK1^{Ser757} (Figures 3A–3C). These results suggested that the SapM-mediated suppression occurred at the early stage of autophagy induction. In order to confirm this inference, the autophagy induction inhibitor 3-methyladenine (3-MA), targeting the Class III PI3K, chloroquine (CQ), and bafilomycin A1 (Baf), which inhibits the fusion of the autophagosome and lysosome, was used in western blotting assays. It was revealed that the LC3II protein levels were similar in the *Ms::SapM and Ms::WT* infected RAW264.7 or THP-1 cells treated with 3-MA (Figures 3D, 3E, and S3A). This finding indicated that SapM could modulate the initiation of autophagy in *mycobacterial*-infected macrophages. However, despite this, neither CQ (Figures 3F, 3G, and S3B) nor Baf (Figures 3H, 3I, and S3C) could alter the LC3 expression pattern in both *Ms::SapM*-infected and *Ms::WT*-infected RAW264.7 cells. Similar

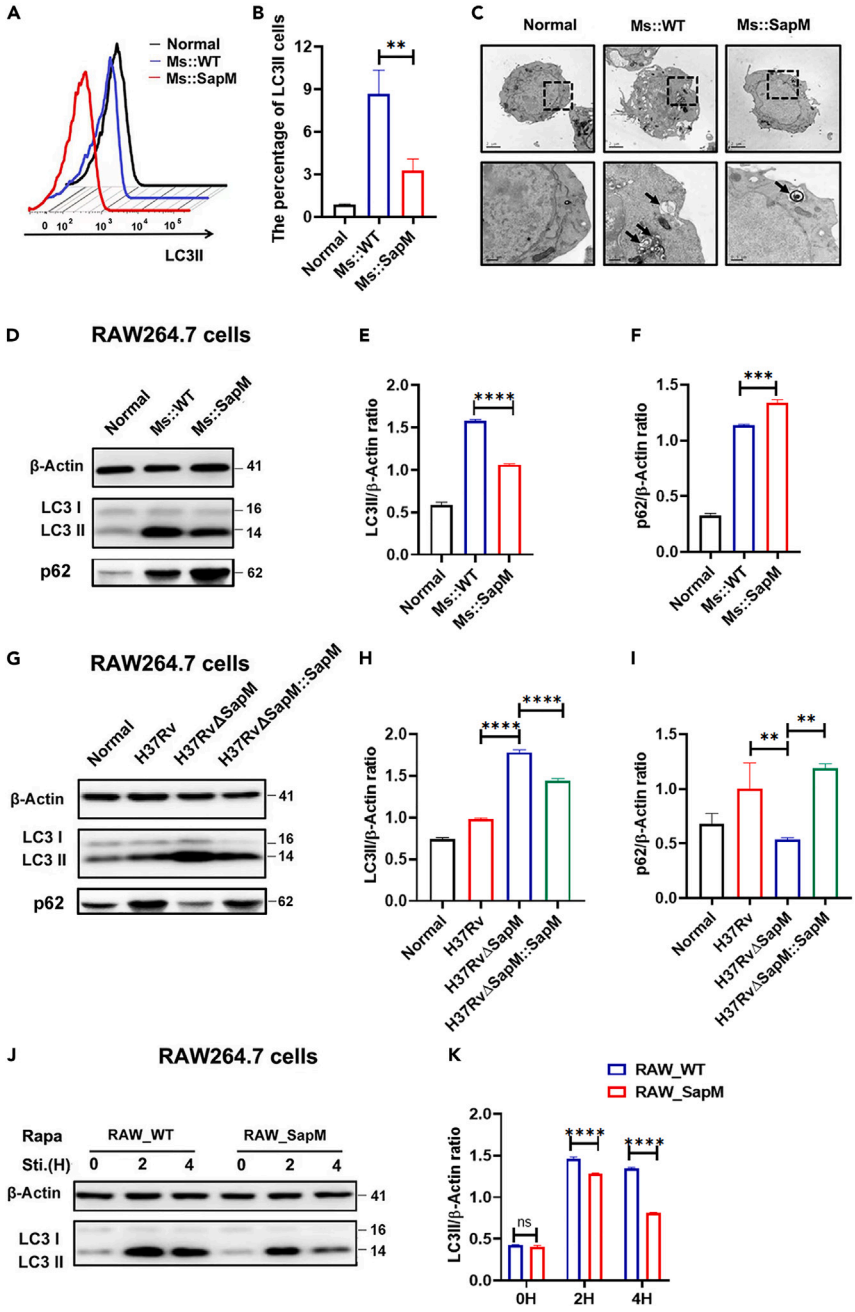

Figure 2. SapM inhibited *mycobacteria*-infected and Rapamycin-induced macrophage autophagy

(A and B) RAW264.7 cells were infected with *Ms::WT* or *Ms::SapM* (MOI = 10) for 4 h, and the LC3II expression was evaluated using the flow cytometry assay.

(C) The autophagosome and autolysosome (black arrows) were detected using transmission electron microscopy (TEM). Scale bar: 1 μm. The magnified view of the corresponding regions depicted inside the box; scale bar: 200 nm.

(D–F) The LC3 and p62 expression was evaluated using immunoblotting.

(G–I) RAW264.7 cells were infected with *H37Rv*, *H37RvΔSapM*, or *H37RvΔSapM::SapM* (MOI = 10) for 4 h, and the LC3 and p62 expression was evaluated using immunoblotting.

(J and K) RAW_WT cells and RAW_SapM cells were stimulated with Rapamycin for 2 h and 4 h, respectively, and the LC3 expression was evaluated using immunoblotting. ns, not significant; $^{**}p < 0.01$; $^{***}p < 0.001$; $^{****}p < 0.0001$. Densitometric quantification of the western blotting results was performed using ImageJ. Statistical analyses were performed in (B, E, F, H, I, and K) using t test. The data presented are mean ± SD and representative of a minimum of three independent experiments.

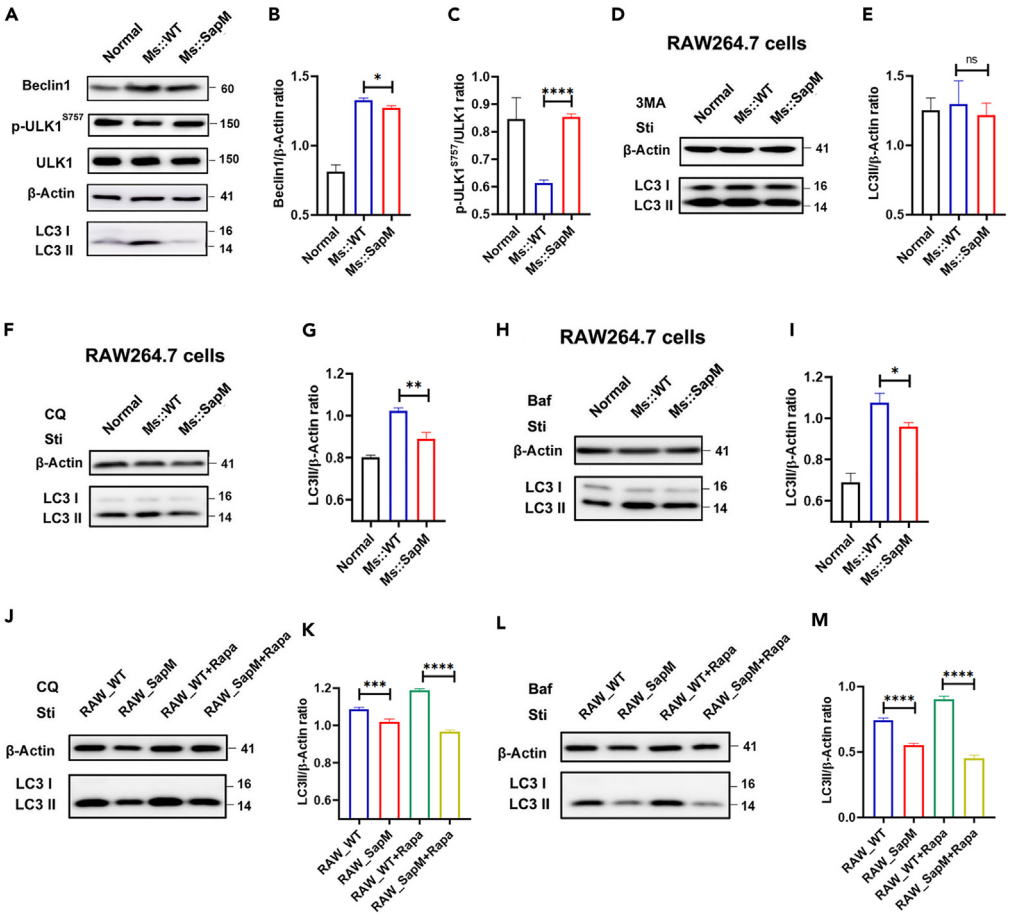

Figure 3. SapM suppressed autophagy induction

(A–C) RAW264.7 cells were infected with *Ms::WT* or *Ms::SapM* (MOI = 10) for 4 h, and the autophagy-related proteins were evaluated using immunoblotting.

(D and E) RAW264.7 cells were treated with 3-MA and then infected with *Ms::WT* or *Ms::SapM* (MOI = 10) for 4 h, followed by the evaluation of LC3 expression using immunoblotting.

(F and G) RAW264.7 cells were treated with CQ and then infected with *Ms::WT* or *Ms::SapM* (MOI = 10) for 4 h, and the LC3 expression was evaluated using immunoblotting.

(H and I) RAW264.7 cells were treated with Baf and then infected with *Ms::WT* or *Ms::SapM* (MOI = 10) for 4 h, followed by the evaluation of LC3 expression using immunoblotting.

(J and K) RAW_WT cells and RAW_SapM cells were stimulated using Rapamycin and CQ, followed by the evaluation of LC3 expression using immunoblotting.

(L and M) RAW_WT cells and RAW_SapM cells were stimulated using Rapamycin and Baf, and the LC3 expression was evaluated using immunoblotting. ns, not significant; *$p < 0.05$; **$p < 0.01$; ***$p < 0.001$; ****$p < 0.0001$. Densitometric quantification of the western blotting results was performed using ImageJ. Statistical analyses were performed in (B, C, E, G, I, K, and M) using t test. The data presented are mean ± SD and representative of a minimum of three independent experiments.

results were observed for the Rapamycin-stimulated RAW_SapM cells and RAW_WT cells with CQ or Baf treatments (Figures 3J–3M). Collectively, these results suggested that SapM served as a suppressor at the autophagy induction stage.

SapM impeded autophagy induction by enhancing mTORC1 activity

The mTORC1 kinase is a widely recognized master modulator of autophagy induction, which governs cell growth. Although SapM is identified as a mycobacterial phosphatase,[25] SapM expression was interestingly observed to increase, rather than decrease, the mTOR phosphorylation levels (Figures 4A and 4B). Accordingly, the mTORC1 activity was observed to increase in the present study, as evidenced by the increased phosphorylation levels of the downstream substrates p70S6 kinase (Figures 4A and 4C) and S6 ribosomal protein (Figures 4D and 4E). Studies have reported the association of small GTPase Rheb and the Rags complex (RagA/B and RagC/D) with mTORC1 activity.[26–29] Accordingly, in the present study, RAW264.7 cells were infected with *Ms::SapM* for different durations, and the cellular localization of SapM was determined (Figure 4F). Co-localization analysis indicated that SapM was co-localized with the lysosome-specific marker LAMP1 in the infected cells as

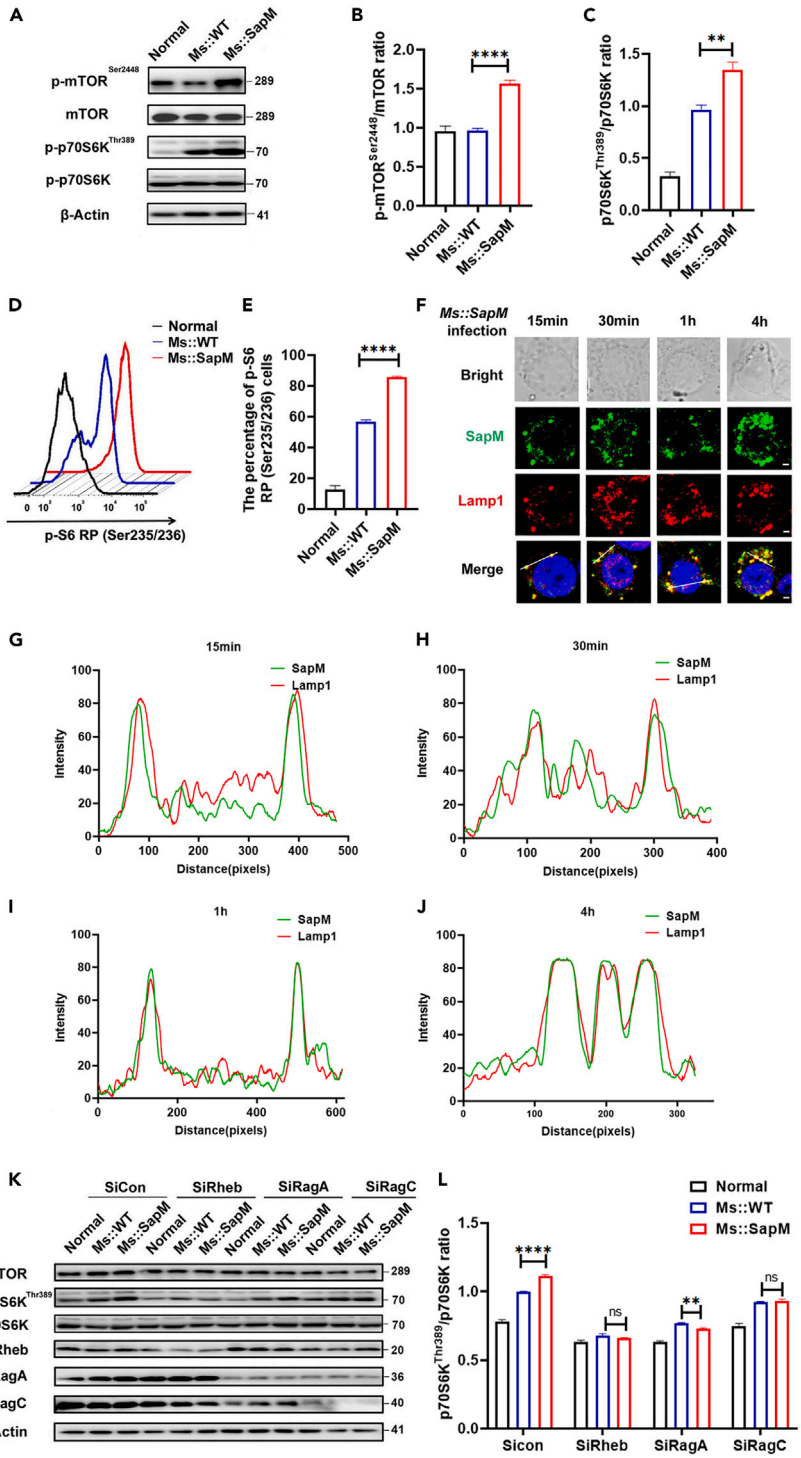

Figure 4. GTPase Rags and Rheb are not the targets of SapM for increasing the mTOR activity

(A–C) RAW264.7 cells were infected with *Ms::WT* and *Ms::SapM* (MOI = 10) for 1 h, followed by the evaluation of mTOR expression and mTORC1 activity using immunoblotting.

(D and E) The detection of p-S6 RP was performed using the flow cytometry assay.

(F–J) RAW264.7 cells were infected with *Ms::SapM* (MOI = 10) for different durations, and the co-localization between the lysosome and SapM was detected using the immunofluorescence assay. Scale bar: 0.5 μm.

Figure 4. *Continued*

(K and L) RAW264.7 cells were transfected with infected siCon, siRagA, siRagC, and siRheb for 36 h and then infected with *Ms::WT* or *Ms::SapM*. Afterward, the mTOR expression and mTORC1 activity were determined using immunoblotting. ns, not significant; $^{**}p < 0.01$; $^{****}p < 0.0001$. Densitometric quantification of the western blotting and confocal results (G–J) were performed using ImageJ. Statistical analyses were performed in (B, C, E, and L) using t test. The data presented are mean ± SD and representative of a minimum of three independent experiments.

early as 15 min post-infection, and this trend continued up to 4 h (Figures 4G–4J). This finding indicated that SapM probably regulated the mTORC1 activity on lysosomes, where SapM probably cooperated with the Rags complex or Rheb. The siRNA experiment indicated that the knockdown of Rheb, RagA, or RagC could not increase the mTORC1 activity (Figures 4K and 4L), which confirmed that GTPase Rags and Rheb are required for SapM-mediated mTORC1 activity enhancement.

SapM increased the mTORC1 activity via dephosphorylating Raptor

Raptor is the main component of the mTORC1 complex, and it interacts with the Rag complex to regulate the mTORC1 activity.[30] In order to validate whether SapM affected the function of Raptor, the interaction between Raptor and SapM was investigated first through the co-immunoprecipitation (Co-IP) assay. The results indicated that SapM could bind to the endogenous Raptor in RAW264.7 cells (Figure 5A). Consistent with this finding, the confocal microscopy images revealed that SapM was suitably co-localized with Raptor (Figures 5B and 5C). Since the phosphorylation level of Raptor is important for suppressing mTORC1 activity,[18] the next step was to determine whether SapM regulated the Raptor phosphorylation levels. While SapM upregulation resulted in increased mTOR phosphorylation levels (Figures 5D and 5E), it was observed to decrease the phosphorylation of Raptor^{Ser792} in RAW_SapM cells compared to RAW_WT cells (Figures 5D and 5F). This effect was similar to that observed under starvation conditions and EBSS treatment (Figures 5G–5I). In addition, the *Ms::SapM*-infected cells exhibited impaired Raptor phosphorylation levels compared to the control group (Figures 5J and 5K), while the mTORC1 activity was increased in the former, as evidenced by the increased levels of phosphorylated p70S6K (Figures 5J–5L). These results suggested that SapM dephosphorylated Raptor, leading to greater binding of Raptor to mTORC1 and increased mTORC1 activation.

SapM alleviated the lung pathological progression in the infected mice

In order to further investigate the SapM-mediated autophagy suppression *in vivo*, a mouse model of *Ms::WT* or *Ms::SapM* was established via intranasal infection (Figure 6A). The western blotting results revealed that compared to the control group, the *Ms::SapM* infected mice group exhibited evidently decreased degree of autophagy in the lung tissue (Figures 6B and 6C). Alveolar macrophages (AMs) are considered tissue-resident macrophages and crucial in the early stages of *Mtb* infection because they are the first cells to phagocytize *Mtb* after inhalation. Previous studies identified that the phenotype of AMs is $CD45^+CD11b^{-/lo}SiglecF^+CD64^+CD11c^+$.[31,32] Hence, $CD45^+CD11b^{-/lo}SiglecF^+CD64^+CD11c^+$ AMs were isolated, and flow cytometric analysis revealed that SapM significantly inhibited autophagy in these cells with *Ms:WT* infection (Figures 6D and 6E). In addition, the LC3 expression levels in the lung tissue were observed to be lower in the *Ms::SapM*-infected mice compared to the control group (Figure 6F). Notably, the H&E staining results revealed that the mice infected with *Ms::SapM* exhibited a less severe lung pathology, as evidenced by reduced immune cell infiltration (Figure 6G). Overall, these findings demonstrated that SapM hampered the *mycobacterial*-infected host autophagy and subsequently alleviated the pathology progression.

DISCUSSION

Mtb evades the host immune system by secreting numerous virulent factors that interfere with the cellular processes of the host or perturb the host immune response, thereby facilitating pathogen survival or replication. For instance, *Mtb* PPE51 was demonstrated to inhibit autophagy to enhance bacterial survival by suppressing the TLR2-dependent signaling pathway,[33] while PPE68 promoted *Mtb* survival by suppressing the TLR2-MyD88-TRAF6-driven NF-κB and AP-1 inflammatory immune responses.[34] The other previously identified secretory virulent factors include Rv3033, Rv1096, Rv0753c, and PPE36.[35–38] In the present study, *Mycobacterial* SapM was observed to strongly facilitate *mycobacterial* survival in *mycobacteria*-infected macrophages via inhibiting autophagy induction, as evidenced by the overall increase in the bacillary loads in infected macrophages, which was consistent with previous reports.[39–41]

Mtb is an intracellular pathogen that evades host immunity, notably within the AMs, during the initial stages of host defense response.[42,43] Upon infecting the host cell, *Mtb* is engulfed by and constrained within the intracellular vacuoles of host macrophages, referred to as phagosomes, which subsequently fuse with the lysosome to form an oxidative and acidic phagolysosome in which degradation occurs.[44] However, *Mtb* has developed sophisticated secretory systems (ESX, SecA, and Tat) to evade the host defense system. The secreted *mycobacterial* components modulate a series of cellular processes, including phagosome processes, autophagy, apoptosis, and inflammation, to facilitate efficient *Mtb* replication.[45] Previously, our research group observed that Rv0790c inhibited the early stage of autophagy and promoted bacillary survival.[24] Other reported studies have also demonstrated that the *Mtb* virulence factors named lipid thiosolipid[46] and LprE[47] regulate early stage autophagy to enhance bacterial survival within the macrophages, while PE_PGRS47 and PE_PGRS41 were reported to be involved in the autophagosome formation stage.[48,49] Interestingly, our findings consistently demonstrated SapM mediated inhibition across multiple cells including RAW264.7, BMDM, THP-1, and human MDMs. Furthermore, we observed that the impairment of autophagy induction mediated by SapM could be effectively blocked with 3-MA treatment but not with CQ or Baf

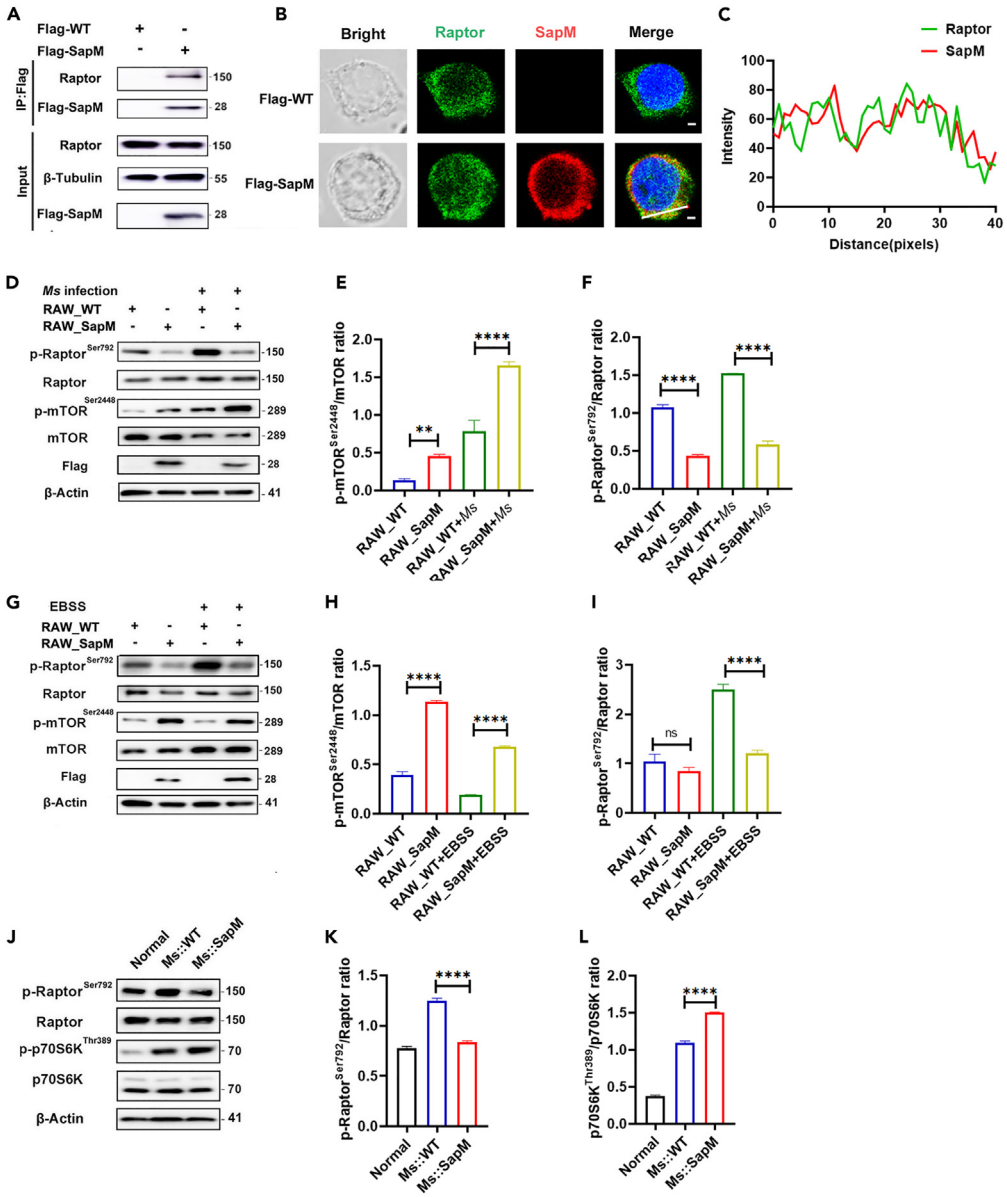

Figure 5. SapM interacted with Raptor and dephosphorylated Raptor

(A) RAW264.7 cells were stably transfected with Flag-WT or Flag-SapM, followed by the detection of interaction between endogenous Raptor and SapM using immunoblotting and the immunoprecipitation assay.

(B and C) The co-localization between SapM and Raptor was detected using the immunofluorescence assay. Scale bar: 0.5 μm.

(D–F) RAW_WT cells and RAW_SapM cells were infected with *Ms* (MOI = 10) or (G–I.) incubated in the culture medium with or without EBSS for 1 h, followed by the evaluation of p-Raptor^{Ser792}, Raptor, mTOR^{Ser2448}, and mTOR expressions using immunoblotting.

(J–L) RAW264.7 cells were infected with *Ms::WT* and *Ms::SapM* (MOI = 10) for 1h, followed by the evaluation of p-Raptor^{Ser792}, Raptor, p70S6K^{Thr389}, p70S6K, mTOR^{Ser2448}, and mTOR expressions using immunoblotting. IB, immunoblotting; IP, immunoprecipitation. ns, not significant; $^{**}p < 0.01$; $^{****}p < 0.0001$. Densitometric quantification of the western blotting and confocal results(C) were performed using ImageJ. Statistical analyses were performed in (E, F, H, I, K, and L) using t test. The data presented are mean ± SD and representative of a minimum of three independent experiments.

treatment. This suggests that SapM may specifically affect autophagy at the early stage of induction. Notably, this inference differs from the previous report by Dong Hu et al., who proposed that SapM exerts its inhibitory effect on autophagosome-lysosome fusion through binding with RAB7.[50]

The mTORC1-dependent canonical autophagy is a widely recognized process of the effective elimination of *Mtb*. However, *Mtb* secretes multiple proteins, such as Eis, ESAT6, HBHA, etc., to modulate the mTORC1-mediated autophagy pathway and promote intracellular bacillary

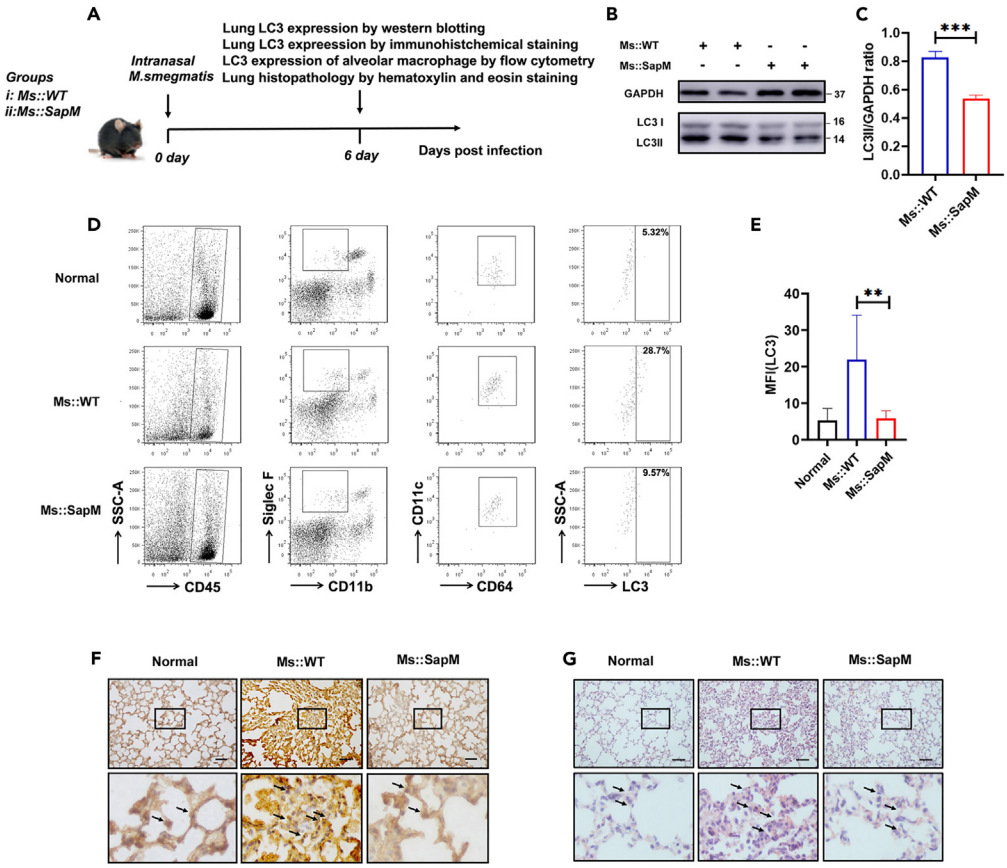

Figure 6. SapM decreased the degree of autophagy and alleviated lung pathology progression in *Ms*-infected mice

(A) Schematic diagram illustrating the mouse intranasal model of *Ms* infection. The C57BL/6 mice were intranasally infected with *Ms::WT* and *Ms::SapM* for 6 days.

(B and C) The LC3 expression in the lung of each mouse was evaluated using immunoblotting.

(D and E) The LC3 expression in the alveolar macrophages was evaluated using the flow cytometry assay.

(F) The LC3 expression in the lung of each mouse was evaluated using the immunohistochemistry assay. The black arrows indicate LC3. Scale bar: 50 μm.

(G) Histopathology of the lung tissue stained with hematoxylin and eosin. The black arrows indicate cellular infiltration. Scale bar: 50 μm. $^{**}p < 0.01$; $^{***}p < 0.001$. Densitometric quantification of the western blotting was performed using ImageJ. Statistical analyses were performed in (C and E) using t test. The data presented are mean ± SD and representative of a minimum of three independent experiments.

survival.[51–53] Several recent studies have revealed that regulating mTORC1-mediated autophagy facilitates limiting *Mtb* survival, and mTOR inhibitors have been approved as attractive targets for the HDT approach of treatment.[54] The lipid phosphatase PTEN reportedly mitigates *Mtb* infection by inhibiting the PI3K-Akt-mTOR signaling pathway in MCF-7 cells.[55] Baicalin, on the other hand, inhibits mTOR-mediated autophagy through the phosphorylation of Akt and resists intracellular *Mtb*.[56] TRIM16 induces mTOR-mediated autophagy by combining with galectin-3 to recognize the damaged phagosomes, thereby inhibiting *Mtb* survival.[57] In our study, due to SapM suppressed *mycobacterial*-infected autophagy induction, we examined the expression of mTOR and p70S6K, two key proteins involved in autophagy initiation. Surprisingly, despite being a phosphatase, SapM did not reduce the phosphorylation of mTOR; instead, it promoted its phosphorylation. Additionally, we observed the phosphorylation of p70S6K increased upon SapM expression. These findings suggest that SapM affects autophagy initiation and enhances mTOR activity, but it does not directly reduce the phosphorylation level of mTOR. Furthermore, Raptor, a main component of the mTORC1 complex that interacts with the Rag complex to regulate mTORC1 activity, was investigated. Interestingly, we found that SapM decreased Raptor phosphorylation level at Ser792 residue under both starvation conditions and *mycobacterial* infection, which resulted in weakened autophagy induction. It ultimately favored *Mtb* survival within host cells. Further investigation is, however, warranted to determine whether Raptor could be a potential target for the HDT approach of treatment for *Mtb*.

In conclusion, the present study revealed that in *Mtb*-infected cells, *mycobacterial* SapM enhances the mTORC1 activity through interactions with Raptor and dephosphorylation of Raptor Ser792, which results in the suppression of early autophagy induction. Future research should focus on determining the efficacy of SapM as a therapeutic target for TB treatment.

Limitations of the study

In this investigation, we have elucidated that SapM impedes autophagy by augmenting mTORC1 activity via its interaction with Raptor and dephosphorylation of Raptor Ser792. However, our study has some limitations. Firstly, we established *H37Rv*-knockout SapM strain (*H37RvΔSapM*) and its rescue strain (*H37RvΔSapM*::*SapM*) and utilized these strains to investigate bacillary survival *in vitro*. Due to the biosafety level, we could not perform the *H37Rv* infection in animal models. Secondly, further experiments are needed to investigate how the dephosphorylation of Raptor affects its function. Thirdly, more clinical data should be explored to investigate the relevance of SapM with TB outcome. The inclusion of clinical data would enhance the findings.

STAR★METHODS

Detailed methods are provided in the online version of this paper and include the following:

- KEY RESOURCES TABLE
- RESOURCE AVAILABILITY
  - Lead contact
  - Materials availability
  - Data and code availability
- EXPERIMENTAL MODEL AND STUDY PARTICIPANT DETAILS
  - Cells culture
  - Mouse infection model
- METHOD DETAILS
  - Plasmid construction
  - Construction of the recombinant M. smegmatis strains and bacterial culture
  - Construction of stable cell lines RAW_WT and RAW_SapM
  - Flow cytometry
  - Immunofluorescence assays
  - Scanning electron microscopy (SEM)
  - Immunoprecipitation assays
  - Immunoblotting assays
  - Intracellular survival
- QUANTIFICATION AND STATISTICAL ANALYSIS

SUPPLEMENTAL INFORMATION

Supplemental information can be found online at https://doi.org/10.1016/j.isci.2024.109671.

ACKNOWLEDGMENTS

This work was supported by the National Natural Science Foundation of China under grants (82101848, 32170927, 32170148, and 82371813), Suzhou International Joint Laboratory for Diagnosis and Treatment of Brain Diseases, and by Jiangsu Provincial Innovative Research Team, the Priority Academic Program Development of Jiangsu Higher Education Institutions.

AUTHOR CONTRIBUTIONS

W.Z. and C.D. designed experiments, performed the animal experiments and the *in vitro* experiments, analyzed data, and wrote the manuscript. C.D. and S.X. reviewed and revising the manuscript article. All authors reviewed and approved the final version of the manuscript.

DECLARATION OF INTERESTS

The authors declare no competing interests.

Received: November 26, 2023
Revised: February 1, 2024
Accepted: April 2, 2024
Published: April 5, 2024

REFERENCES

1. WHO (2023). Global Tuberculosis Report (Global report World Health Organization (WHO)).
2. Pai, M., Behr, M.A., Dowdy, D., Dheda, K., Divangahi, M., Boehme, C.C., Ginsberg, A., Swaminathan, S., Spigelman, M., Getahun, H., et al. (2016). Tuberculosis. Nat. Rev. Dis. Prim. *2*, 16076. https://doi.org/10.1038/nrdp.2016.76.
3. Kilinç, G., Saris, A., Ottenhoff, T.H.M., and Haks, M.C. (2021). Host-directed therapy to combat mycobacterial infections. Immunol. Rev. *301*, 62–83. https://doi.org/10.1111/imr.12951.
4. Strong, E.J., and Lee, S. (2020). Targeting Autophagy as a Strategy for Developing New Vaccines and Host-Directed Therapeutics Against Mycobacteria. Front. Microbiol. *11*, 614313. https://doi.org/10.3389/fmicb.2020.614313.
5. Racanelli, A.C., Kikkers, S.A., Choi, A.M.K., and Cloonan, S.M. (2018). Autophagy and inflammation in chronic respiratory disease. Autophagy *14*, 221–232. https://doi.org/10.1080/15548627.2017.1389823.
6. Paik, S., and Jo, E.K. (2020). An Interplay Between Autophagy and Immunometabolism for Host Defense Against Mycobacterial Infection. Front. Immunol. *11*, 603951. https://doi.org/10.3389/fimmu.2020.603951.
7. Sachan, M., Srivastava, A., Ranjan, R., Gupta, A., Pandya, S., and Misra, A. (2016). Opportunities and Challenges for Host-Directed Therapies in Tuberculosis. Curr. Pharmaceut. Des. *22*, 2599–2604. https://doi.org/10.2174/1381612822666160128150636.
8. Andersson, A.M., Andersson, B., Lorell, C., Raffetseder, J., Larsson, M., and Blomgran, R. (2016). Autophagy induction targeting mTORC1 enhances Mycobacterium tuberculosis replication in HIV co-infected human macrophages. Sci. Rep. *6*, 28171. https://doi.org/10.1038/srep28171.
9. Mizushima, N., and Komatsu, M. (2011). Autophagy: renovation of cells and tissues. Cell *147*, 728–741. https://doi.org/10.1016/j.cell.2011.10.026.
10. Galluzzi, L., Baehrecke, E.H., Ballabio, A., Boya, P., Bravo-San Pedro, J.M., Cecconi, F., Choi, A.M., Chu, C.T., Codogno, P., Colombo, M.I., et al. (2017). Molecular definitions of autophagy and related processes. EMBO J. *36*, 1811–1836. https://doi.org/10.15252/embj.201796697.
11. Mazure, N.M., and Pouysségur, J. (2010). Hypoxia-induced autophagy: cell death or cell survival? Curr. Opin. Cell Biol. *22*, 177–180. https://doi.org/10.1016/j.ceb.2009.11.015.
12. Shi, X., Chen, Z., Tang, S., Wu, F., Xiong, S., and Dong, C. (2016). Coxsackievirus B3 infection induces autophagic flux, and autophagosomes are critical for efficient viral replication. Arch. Virol. *161*, 2197–2205. https://doi.org/10.1007/s00705-016-2896-6.
13. Zachari, M., and Ganley, I.G. (2017). The mammalian ULK1 complex and autophagy initiation. Essays Biochem. *61*, 585–596. https://doi.org/10.1042/EBC20170021.
14. Yang, H., Jiang, X., Li, B., Yang, H.J., Miller, M., Yang, A., Dhar, A., and Pavletich, N.P. (2017). Mechanisms of mTORC1 activation by RHEB and inhibition by PRAS40. Nature *552*, 368–373. https://doi.org/10.1038/nature25023.
15. Kim, J., Kundu, M., Viollet, B., and Guan, K.L. (2011). AMPK and mTOR regulate autophagy through direct phosphorylation of Ulk1. Nat. Cell Biol. *13*, 132–141. https://doi.org/10.1038/ncb2152.
16. Takahara, T., Amemiya, Y., Sugiyama, R., Maki, M., and Shibata, H. (2020). Amino acid-dependent control of mTORC1 signaling: a variety of regulatory modes. J. Biomed. Sci. *27*, 87. https://doi.org/10.1186/s12929-020-00679-2.
17. Van Nostrand, J.L., Hellberg, K., Luo, E.C., Van Nostrand, E.L., Dayn, A., Yu, J., Shokhirev, M.N., Dayn, Y., Yeo, G.W., and Shaw, R.J. (2020). AMPK regulation of Raptor and TSC2 mediate metformin effects on transcriptional control of anabolism and inflammation. Genes Dev. *34*, 1330–1344. https://doi.org/10.1101/gad.339895.120.
18. Gwinn, D.M., Shackelford, D.B., Egan, D.F., Mihaylova, M.M., Mery, A., Vasquez, D.S., Turk, B.E., and Shaw, R.J. (2008). AMPK phosphorylation of raptor mediates a metabolic checkpoint. Mol. Cell *30*, 214–226. https://doi.org/10.1016/j.molcel.2008.03.003.
19. Pisu, D., Huang, L., Grenier, J.K., and Russell, D.G. (2020). Dual RNA-Seq of Mtb-Infected Macrophages In Vivo Reveals Ontologically Distinct Host-Pathogen Interactions. Cell Rep. *30*, 335–350.e4. https://doi.org/10.1016/j.celrep.2019.12.033.
20. Wong, D., Chao, J.D., and Av-Gay, Y. (2013). Mycobacterium tuberculosis-secreted phosphatases: from pathogenesis to targets for TB drug development. Trends Microbiol. *21*, 100–109. https://doi.org/10.1016/j.tim.2012.09.002.
21. Cadwell, K. (2016). Crosstalk between autophagy and inflammatory signalling pathways: balancing defence and homeostasis. Nat. Rev. Immunol. *16*, 661–675. https://doi.org/10.1038/nri.2016.100.
22. Ge, P., Lei, Z., Yu, Y., Lu, Z., Qiang, L., Chai, Q., Zhang, Y., Zhao, D., Li, B., Pang, Y., et al. (2022). M. tuberculosis PknG manipulates host autophagy flux to promote pathogen intracellular survival. Autophagy *18*, 576–594. https://doi.org/10.1080/15548627.2021.1938912.
23. Shin, D.M., Jeon, B.Y., Lee, H.M., Jin, H.S., Yuk, J.M., Song, C.H., Lee, S.H., Lee, Z.W., Cho, S.N., Kim, J.M., et al. (2010). Mycobacterium tuberculosis eis regulates autophagy, inflammation, and cell death through redox-dependent signaling. PLoS Pathog. *6*, e1001230. https://doi.org/10.1371/journal.ppat.1001230.
24. Fang, J., Dong, C., and Xiong, S. (2022). Mycobacterium tuberculosis Rv0790c inhibits the cellular autophagy at its early stage and facilitates mycobacterial survival. Front. Cell. Infect. Microbiol. *12*, 1014897. https://doi.org/10.3389/fcimb.2022.1014897.
25. Saleh, M.T., and Belisle, J.T. (2000). Secretion of an acid phosphatase (SapM) by Mycobacterium tuberculosis that is similar to eukaryotic acid phosphatases. J. Bacteriol. *182*, 6850–6853. https://doi.org/10.1128/JB.182.23.6850-6853.2000.
26. Bar-Peled, L., and Sabatini, D.M. (2012). SnapShot: mTORC1 signaling at the lysosomal surface. Cell *151*, 1390–1390.e1. https://doi.org/10.1016/j.cell.2012.11.038.
27. Demetriades, C., Doumpas, N., and Teleman, A.A. (2014). Regulation of TORC1 in response to amino acid starvation via lysosomal recruitment of TSC2. Cell *156*, 786–799. https://doi.org/10.1016/j.cell.2014.01.024.
28. Sabatini, D.M. (2017). Twenty-five years of mTOR: Uncovering the link from nutrients to growth. Proc. Natl. Acad. Sci. USA *114*, 11818–11825. https://doi.org/10.1073/pnas.1716173114.
29. Rogala, K.B., Gu, X., Kedir, J.F., Abu-Remaileh, M., Bianchi, L.F., Bottino, A.M.S., Dueholm, R., Niehaus, A., Overwijn, D., Fils, A.C.P., et al. (2019). Structural basis for the docking of mTORC1 on the lysosomal surface. Science *366*, 468–475. https://doi.org/10.1126/science.aay0166.
30. Sancak, Y., Peterson, T.R., Shaul, Y.D., Lindquist, R.A., Thoreen, C.C., Bar-Peled, L., and Sabatini, D.M. (2008). The Rag GTPases bind raptor and mediate amino acid signaling to mTORC1. Science *320*, 1496–1501. https://doi.org/10.1126/science.1157535.
31. DiPiazza, A., Nogales, A., Poulton, N., Wilson, P.C., Martínez-Sobrido, L., and Sant, A.J. (2017). Pandemic 2009 H1N1 Influenza Venus reporter virus reveals broad diversity of MHC class II-positive antigen-bearing cells following infection *in vivo*. Sci. Rep. *7*, 10857. https://doi.org/10.1038/s41598-017-11313-x.
32. Misharin, A.V., Morales-Nebreda, L., Mutlu, G.M., Budinger, G.R.S., and Perlman, H. (2013). Flow cytometric analysis of macrophages and dendritic cell subsets in the mouse lung. Am. J. Respir. Cell Mol. Biol. *49*, 503–510. https://doi.org/10.1165/rcmb.2013-0086MA.
33. Strong, E.J., Wang, J., Ng, T.W., Porcelli, S.A., and Lee, S. (2022). Mycobacterium tuberculosis PPE51 Inhibits Autophagy by Suppressing Toll-Like Receptor 2-Dependent Signaling. mBio *13*, e0297421. https://doi.org/10.1128/mbio.02974-21.
34. Dou, Y., Xie, Y., Zhang, L., Liu, S., Xu, D., Wei, Y., Li, Y., and Zhang, X.L. (2022). Host MKRN1-Mediated Mycobacterial PPE Protein Ubiquitination Suppresses Innate Immune Response. Front. Immunol. *13*, 880315. https://doi.org/10.3389/fimmu.2022.880315.
35. Zhang, W., Lu, Q., Dong, Y., Yue, Y., and Xiong, S. (2018). Rv3033, as an Emerging Anti-apoptosis Factor, Facilitates Mycobacteria Survival via Inhibiting Macrophage Intrinsic Apoptosis. Front. Immunol. *9*, 2136. https://doi.org/10.3389/fimmu.2018.02136.
36. Lu, Q., Zhang, W., Fang, J., Zheng, J., Dong, C., and Xiong, S. (2020). Mycobacterium tuberculosis Rv1096, facilitates mycobacterial survival by modulating the NF-kappaB/MAPK pathway as peptidoglycan N-deacetylase. Mol. Immunol. *127*, 47–55. https://doi.org/10.1016/j.molimm.2020.08.005.
37. Sun, Y., Zhang, W., Dong, C., and Xiong, S. (2020). Mycobacterium tuberculosis MmsA (Rv0753c) interacts with STING and blunts the type I interferon response. mBio *11*, e03254-19. https://doi.org/10.1128/mBio.03254-19.
38. Peng, Z., Yue, Y., and Xiong, S. (2022). Mycobacterial PPE36 Modulates Host Inflammation by Promoting E3 Ligase Smurf1-Mediated MyD88 Degradation. Front. Immunol. *13*, 690667. https://doi.org/10.3389/fimmu.2022.690667.
39. Puri, R.V., Reddy, P.V., and Tyagi, A.K. (2013). Secreted acid phosphatase (SapM) of Mycobacterium tuberculosis is indispensable for arresting phagosomal maturation and growth of the pathogen in guinea pig tissues. PLoS One *8*, e70514. https://doi.org/10.1371/journal.pone.0070514.

40. Saikolappan, S., Estrella, J., Sasindran, S.J., Khan, A., Armitige, L.Y., Jagannath, C., and Dhandayuthapani, S. (2012). The fbpA/sapM double knock out strain of Mycobacterium tuberculosis is highly attenuated and immunogenic in macrophages. PLoS One *7*, e36198. https://doi.org/10.1371/journal.pone.0036198.
41. Chauhan, P., Reddy, P.V., Singh, R., Jaisinghani, N., Gandotra, S., and Tyagi, A.K. (2013). Secretory phosphatases deficient mutant of Mycobacterium tuberculosis imparts protection at the primary site of infection in guinea pigs. PLoS One *8*, e77930. https://doi.org/10.1371/journal.pone.0077930.
42. Chai, Q., Lu, Z., and Liu, C.H. (2020). Host defense mechanisms against Mycobacterium tuberculosis. Cell. Mol. Life Sci. *77*, 1859–1878. https://doi.org/10.1007/s00018-019-03353-5.
43. Chai, Q., Wang, L., Liu, C.H., and Ge, B. (2020). New insights into the evasion of host innate immunity by. Cell. Mol. Immunol. *17*, 901–913. https://doi.org/10.1038/s41423-020-0502-z.
44. Bussi, C., and Gutierrez, M.G. (2019). Mycobacterium tuberculosis infection of host cells in space and time. FEMS Microbiol. Rev. *43*, 341–361. https://doi.org/10.1093/femsre/fuz006.
45. Pajuelo, D., Tak, U., Zhang, L., Danilchanka, O., Tischler, A.D., and Niederweis, M. (2021). Toxin secretion and trafficking by Mycobacterium. Nat. Commun. *12*, 6592. https://doi.org/10.1038/s41467-021-26925-1.
46. Bah, A., Sanicas, M., Nigou, J., Guilhot, C., Astarie-Dequeker, C., and Vergne, I. (2020). The Lipid Virulence Factors of Mycobacterium tuberculosis Exert Multilayered Control over Autophagy-Related Pathways in Infected Human Macrophages. Cells *9*, 666. https://doi.org/10.3390/cells9030666.
47. Padhi, A., Pattnaik, K., Biswas, M., Jagadeb, M., Behera, A., and Sonawane, A. (2019). Mycobacterium tuberculosis LprE suppresses TLR2-dependent cathelicidin and autophagy expression to enhance bacterial survival in macrophages. J. Immunol. *203*, 2665–2678. https://doi.org/10.4049/jimmunol.1801301.
48. Deng, W., Long, Q., Zeng, J., Li, P., Yang, W., Chen, X., and Xie, J. (2017). Mycobacterium tuberculosis PE_PGRS41 Enhances the Intracellular Survival of M. smegmatis within Macrophages Via Blocking Innate Immunity and Inhibition of Host Defense. Sci. Rep. *7*, 46716. https://doi.org/10.1038/srep46716.
49. Saini, N.K., Baena, A., Ng, T.W., Venkataswamy, M.M., Kennedy, S.C., Kunnath-Velayudhan, S., Carreño, L.J., Xu, J., Chan, J., Larsen, M.H., et al. (2016). Suppression of autophagy and antigen presentation by Mycobacterium tuberculosis PE_PGRS47. Nat. Microbiol. *1*, 16133. https://doi.org/10.1038/nmicrobiol.2016.133.
50. Hu, D., Wu, J., Wang, W., Mu, M., Zhao, R., Xu, X., Chen, Z., Xiao, J., Hu, F., Yang, Y., and Zhang, R. (2015). Autophagy regulation revealed by SapM-induced block of autophagosome-lysosome fusion via binding RAB7. Biochem. Biophys. Res. Commun. *461*, 401–407. https://doi.org/10.1016/j.bbrc.2015.04.051.
51. Duan, L., Yi, M., Chen, J., Li, S., and Chen, W. (2016). Mycobacterium tuberculosis EIS gene inhibits macrophage autophagy through up-regulation of IL-10 by increasing the acetylation of histone H3. Biochem. Biophys. Res. Commun. *473*, 1229–1234. https://doi.org/10.1016/j.bbrc.2016.04.045.
52. Dong, H., Jing, W., Runpeng, Z., Xuewei, X., Min, M., Ru, C., Yingru, X., Shengfa, N., and Rongbo, Z. (2016). ESAT6 inhibits autophagy flux and promotes BCG proliferation through MTOR. Biochem. Biophys. Res. Commun. *477*, 195–201. https://doi.org/10.1016/j.bbrc.2016.06.042.
53. Zheng, Q., Li, Z., Zhou, S., Zhang, Q., Zhou, L., Fu, X., Yang, L., Ma, Y., and Hao, X. (2017). Heparin-binding hemagglutinin of mycobacterium tuberculosis Is an inhibitor of autophagy. Front. Cell. Infect. Microbiol. *7*, 33. https://doi.org/10.3389/fcimb.2017.00033.
54. Singh, P., and Subbian, S. (2018). Harnessing the mTOR Pathway for Tuberculosis Treatment. Front. Microbiol. *9*, 70. https://doi.org/10.3389/fmicb.2018.00070.
55. Huang, G., Redelman-Sidi, G., Rosen, N., Glickman, M.S., and Jiang, X. (2012). Inhibition of mycobacterial infection by the tumor suppressor PTEN. J. Biol. Chem. *287*, 23196–23202. https://doi.org/10.1074/jbc.M112.351940.
56. Zhang, Q., Sun, J., Wang, Y., He, W., Wang, L., Zheng, Y., Wu, J., Zhang, Y., and Jiang, X. (2017). Antimycobacterial and Anti-inflammatory Mechanisms of Baicalin via Induced Autophagy in Macrophages Infected with Mycobacterium tuberculosis. Front. Microbiol. *8*, 2142. https://doi.org/10.3389/fmicb.2017.02142.
57. Chauhan, S., Kumar, S., Jain, A., Ponpuak, M., Mudd, M.H., Kimura, T., Choi, S.W., Peters, R., Mandell, M., Bruun, J.A., et al. (2016). TRIMs and Galectins Globally Cooperate and TRIM16 and Galectin-3 Co-direct Autophagy in Endomembrane Damage Homeostasis. Dev. Cell *39*, 13–27. https://doi.org/10.1016/j.devcel.2016.08.003.

STAR★METHODS

KEY RESOURCES TABLE

REAGENT or RESOURCE	SOURCE	IDENTIFIER
Antibodies		
Anti-mTOR	Cell Signaling Technology	Cat# 2972
Anti-Phospho-mTOR (Ser2448)	Cell Signaling Technology	Cat# 2971
Anti-p70S6Kinase	Cell Signaling Technology	Cat# 9202
Anti-Phospho-p70S6Kinase (Thr389)	Cell Signaling Technology	Cat# 9234
Anti-Beclin1	Cell Signaling Technology	Cat# 3495
Anti-p62	Cell Signaling Technology	Cat# 5114
Anti-ULK1	Cell Signaling Technology	Cat# 8054
Anti-Phospho-ULK1(Ser757)	Cell Signaling Technology	Cat# 14202
Anti-β-actin	Cell Signaling Technology	Cat# 3700
Anti-GADPH	ABclonal Technology	Cat# AC001
Anti-β-tubulin	ABclonal Technology	Cat# AC015
Anti-RagA	ABclonal Technology	Cat# A7771
Anti-RagC	ABclonal Technology	Cat# A7479
Anti-Rheb	ABclonal Technology	Cat# A1165
Anti-Phospho-Raptor(Ser792)	ABclonal Technology	Cat# AP0928
Anti-Raptor	ABclonal Technology	Cat# A8992
Anti-LC3	Sigma-Aldrich	Cat#L7543
Anti-Flag	Sigma-Aldrich	Cat# F7425; RRID:AB_439687
HRP-conjugated goat anti-mouse IgG	Southern-Biotech	Cat# 1091-05
HRP-conjugated goat anti-rabbit IgG	Southern-Biotech	Cat# 4030-05
Anti-SapM	This study	N/A
DyLight 633-labeled antibody to rabbit IgG	Jackson	Cat# 111-605-144
DyLight 488-labeled antibody to mouse IgG	Jackson	Cat# 111-545-003
Recombinant DNA		
pMV261	Honghai Wang	N/A
pMV261-SapM	This study	N/A
pMV261-mCherry	Gene Optimal	N/A
pMV261-mCherry-SapM	This study	N/A
pFLAG-CMV2	This study	N/A
pFLAG-CMV2-SapM	This study	N/A
pMSCV-eGFP	Jinping Zhang	N/A
pMSCV-eGFP-SapM	This study	N/A
pcl-Ampho	Hui Zheng	N/A
pET28a	This study	N/A
pET28a-SapM	This study	N/A
Oligonucleotides		
pMV261-SapM-F C-tag BamH I	Genewiz	CATGGATCCATGCTCCGCGGAATCCAGGCTCTCA
pMV261-SapM-R C-tag HINDIII	Genewiz	CAGAAGCTTCTACTTGTCGTCATCGTCTTTGT AGTCCAT GTCGCCCCAAATATCGGTTAT
pMV261-mCherry-SapM-F BamH I	Genewiz	CGCGCGGATCCATGCTCCGCGGAATCCAG

(*Continued on next page*)

Continued

REAGENT or RESOURCE	SOURCE	IDENTIFIER
pMV261-mCherry-SapM-R EcoRI	Genewiz	CCGGAATTCCTTGTCGTCATCGTCTTTGTA GTCGTCGCCCCAAATATCGGTTAT
pFLAG-CMV2-SapM-F HINDIII	Genewiz	CCCAAGCTTGCGAGTGCCCTGCCGAC
pFLAG-CMV2-SapM-R BamHI	Genewiz	CGCGGATCCCTAGTCGCCCCAAATATCGGTTA
pMSCV-eGFP-SapM-F XhoI	Genewiz	CCGCTCGAGATGGACTACAAAGACGATGAC GACAAGCTGCCGACCTTCGCGCACGTGGTCAT
pMSCV-eGFP-SapM-R HpaI	Genewiz	AAGGTTAACCTAGTCGCCCCAAATATCGGTTAT
pET28a-SapM-F BamHI	Genewiz	CATGGATCCATGCTCCGCGGAATCCAGGCTCTCA
pET28a-SapM-R XhoI	Genewiz	CATCTCGAGCTAGTCGCCCCAAATATCGGTTAT
SiRagA-mouse	Ribobio	GGGACAACATCTTCCGTAA
SiRagC-mouse	Ribobio	GCACTGGTTTGCATTCTTA
SiRheb-mouse	Ribobio	GGAAAGTCCTCATTGACAA
SiRaptor-mouse	Ribobio	TCCTCAACAGCATTGCTTA
Bacterial and virus strains		
DH5α	weidibio	Cat# DL1001
BL21(DE3)	weidibio	Cat# EC1002S
mc^2155	Soochow University, China	Guoping Zhao
H37Rv	Gene Optimal Inc.	N/A
H37RvΔSapM	Gene Optimal Inc.	N/A
*H37RvΔ*SapM::SapM	Gene Optimal Inc.	N/A
Ms::SapM	This study	N/A
Ms::mCherry-SapM	This study	N/A
Chemicals and recombinant proteins		
3-Methyladenine (3-MA)	Sigma	Cat# 5142-23-4
Chloroquine(CQ)	Sigma	Cat# 50-63-5
Bafilomycin A1(Baf)	Sigma	Cat# 88899-55-2
Phorbol 12-myristate 13-acetate (PMA)	Sigma	Cat#16561-29-8
Anti-FLAG M2 affinity gel	Sigma	Cat# A2220
m-CSF	peprotech	Cat# xy-090Ra01
Experimental models: Cell lines		
HEK293T	This study	N/A
RAW264.7	This study	N/A
THP-1	This study	N/A
BMDM	This study	N/A
hMDM	Stemexpress	Cat# PBMAC005C
Experimental models: Organisms/strains		
C57BL/6 mice	Experimental Animal Center of the Chinese Academy of Sciences	N/A
Deposited		
Raw western blot	Mendeley Data	https://doi.org/10.17632/bv5ktdbyj3.1
Raw H&E	Mendeley Data	
Raw FACS	Mendeley Data	
Raw IF	Mendeley Data	
Raw CFU	Mendeley Data	
Other		
Others related to the research	This study	sdxiong@suda.edu.cn

RESOURCE AVAILABILITY

Lead contact

Further information and requests for resources should contact to Prof. Sidong Xiong (sdxiong@suda.edu.cn).

Materials availability

The materials are available upon request.

Data and code availability

- Original western blot , HE , FACS, IF and CFU have been deposited at Mendeley and are publicly available as of the date of publication. The DOI is listed in the key resources table.
- This paper does not report original code.
- Any additional information required to reanalyze the data reported in this paper is available from the lead contact upon request.

EXPERIMENTAL MODEL AND STUDY PARTICIPANT DETAILS

Cells culture

The murine macrophage cell line RAW264.7 and the HEK293T cells were cultured in Dulbecco's modified Eagle's medium (DMEM, Sigma-Aldrich) supplemented with 10% fetal bovine serum (FBS) and 1% penicillin-streptomycin. The THP-1 monocytes were treated with 40 ng/mL of phorbol 12-myristate 13-acetate (PMA) (Sigma-Aldrich) for 72h to induce their differentiation into THP-1-derived macrophages. Bone marrow-derived macrophages (BMDMs) were prepared using a previously described method.[38] human blood monocyte-derived macrophages (hMDMs) were cultured in RPMI1640 supplemented with 10% fetal bovine serum (FBS) and 1% penicillin-streptomycin. All cells were cultured inside a humidified incubator at 37°C and 5% CO_2 conditions.

Mouse infection model

The 6–8-week-old female C57BL/6 mice were procured from the Experimental Animal Center at the Chinese Academy of Sciences (Shanghai, China). All animal experiments were performed in accordance with the guidelines for the Care and Use of Laboratory Animals, Ministry of Health, China (1998), and the protocols used were approved by the Ethics Committee of Soochow University (201910A201). The mice were housed using the standard humane animal husbandry protocols. In the experiments, each mouse was intranasally infected with *Ms::WT*/*Ms::SapM* or *Ms::mcherry-WT*/*Ms::mcherry-SapM* in 30 μL of PBST. On Day 6 after infection, the lungs were retrieved from the mice and weighed. Afterward, the lung tissue was homogenized in 1 mL PBS, and the tissue homogenate was inoculated onto 7H10 agar plates. The colonies were counted after 3–4 weeks of incubation at 37°C. A few of the lung tissue samples were fixed in 10% formalin and then embedded in paraffin, followed by hematoxylin and eosin staining and then incubation with anti-LC3 for pulmonary immunohistochemistry to evaluate the pathological changes in the lung tissue. A few lung tissue samples were subjected to the evaluation of LC3 expression using immunoblotting. The bacterial loads were determined using small-animal imaging (PerkinElmer).

METHOD DETAILS

Plasmid construction

The SapM gene was amplified from *H37Rv* and then cloned into pMV261 or pMV261-mCherry in a frame with a C-terminal Flag-tag. In addition, the SapM gene amplified from *H37Rv* was cloned into pFlag-CMV2 in frame with the N-terminal Flag-tag. Further, the SapM gene amplified from the *H37Rv* genomic DNA was cloned into the pMSCV-eGFP retroviral vector to form pMSCV-eGFP-SapM. All gene primers used in the above experiments are listed in key resources table.

Construction of the recombinant M. smegmatis strains and bacterial culture

The recombinant strains were constructed using *M. smegmatis* mc^2155 (*Ms*). All constructed genes were electroporated into *Ms*. The selected pMV261 (*Ms::WT*), pMV261-SapM (*Ms::SapM*), pMV 261-mCherry (*Ms::mCherry-WT*), and pMV261-mCherry-SapM (*Ms::mCherry-SapM)* were cultured in the Luria-Bertani medium supplemented with 0.05% Tween-80 containing 50 μg/mL kanamycin. The above-stated recombinant strains were identified through immunoblotting using an anti-flag antibody. Mc^2155 was cultured in the Luria-Bertani medium supplemented with 0.05% Tween-80. *H37Rv*, *H37Rv*ΔSapM, and *H37RvΔSapM::SapM* (Gene Optimal) were culture in the Middlebrook 7H9 broth medium supplemented with 10% ADC, 0.5% glycerol, and 0.05% Tween-80 at 37°C. When OD600 reached 1.0, the bacterial culture was 10-fold diluted with 6 gradients. The dilution was further plated on the plates for culture. Then the bacteria number on the plates was counted.

Construction of stable cell lines RAW_WT and RAW_SapM

HEK293T cells were co-transfected with the retroviral expression plasmid pMSCV-eGFP-WT/pMSCV-eGFP-SapM and the packaging vector PCL-Ampho using Lipofectamine 3000 (Invitrogen). The cell culture supernatants were harvested at the time points of 48h and 72h, filtered through a 0.45-μm filter, and concentrated through ultracentrifugation at 20,000 rpm for 2h. The virus culture supernatants thus obtained were

then resuspended in PBS followed by storage at –80°C until to be used. RAW264.7 cells were later infected with these viral supernatants, and after 72h, the GFP-positive cells were sorted using flow cytometry, and SapM expression was verified using immunoblotting analysis. The RAW264.7 cells infected with pMSCV-eGFP-WT and pMSCV-eGFP-SapM viruses were designated as RAW_WT cells and RAW_SapM cells, respectively.

Flow cytometry

RAW264.7 cells were infected with *Ms::WT* or *Ms::SapM* at a multiplicity of infection (MOI)=10 for 4h. The cells were harvested using trypsin followed by rinsing with the PBS containing 0.05% saponin. Afterward, the cells were incubated with the anti-LC3 antibody for 30 min and then with the anti-rabbit IgG 488 for 30 min, followed by two rinses with PBS. In addition, RAW264.7 cells were infected with *Ms::WT* and *Ms::SapM* at (MOI=10) for 1h. The cells were then harvested, fixed, permeabilized (Becton Dickinson), and incubated with the anti-Phospho-S6 Ribosomal Protein (Ser235/236)-PE (CST) for 30 min, followed by two rinses with PBS. Further, C57BL/6 mice were infected with *Ms::WT* or *Ms::SapM* for 6 days. Afterward, the lung was dispersed in the PBS containing 1 mg/mL of collagenase IV (Roche) followed by incubation at 37°C under constant agitation. Next, the cells were stained with $CD45^{+}CD11b^{-/lo}SiglecF^{+}CD64^{+}CD11c^{+}$ for 30 min, followed by fixing and permeabilizing using the BD solution and then incubation with the anti-LC3 antibody for 30 min. Afterward, the cells were incubated with the anti-rabbit IgG 488 for 30 min, followed by three rinses with PBS. Finally, the FACS data were collected using a FACSCanto II flow cytometer (Becton Dickinson).

Immunofluorescence assays

First, RAW264.7 cells were infected with *Ms::SapM* (MOI=10) for different durations (15 min, 30 min, 1h, and 4h). Next, RAW_WT and RAW_SapM were incubated for overnight. All cells were finally stained as described ahead in brief. The cells were fixed using 4% paraformaldehyde and permeabilized using Triton-X-100, followed by blocking with 3% BSA. Next, the cells were placed on coverslips and incubated overnight with the primary antibody (anti-DDDDK-Tag; anti-Lamp1, Anti-Raptor). Afterward, the cells were incubated overnight with the relevant secondary antibody, followed by three washes with PBS. Subsequently, DNA staining with Hoechst was performed for 15 min at room temperature. Finally, the cells were analyzed using a fluorescence microscope (Nicon A1). Image analysis was performed using ImageJ. For colocalization experiments, images for each channel were separately thresholded, and colocalization was defined as at least one pixel of overlap between the two channels. For colocalization of SapM with various markers, the area of SapM colocalizing with each maker was ratioed. Images analysis was carried out with no post-acquisition modifications. For example images, brightness/contrast were adjusted within linear ranges using ImageJ when necessary. Control and experimental conditions were adjusted with the same parameters.

Scanning electron microscopy (SEM)

RAW264.7 cells were infected with *Ms::WT*, *Ms::SapM* (MOI=10) for 4h. Next, each sample of cells was dehydrated using increasing concentrations of ethanol, followed by gradual adsorption on the Epon-Araldite resin and insertion into a straight resin. The samples were then heated at 80°C for 24 h to allow hardening. The hardened samples were then excised into ultrathin sections (70–80 nm) using an ultramicrotome, followed by staining the sections with uranyl acetate and lead citrate and then observation under a TEM.

Immunoprecipitation assays

RAW_WT and RAW_SapM were incubated for overnight, the cells were washed with cold PBS and then lysed using the western and IP lysis buffer and PMSF. The obtained cell lysates were incubated overnight with EZviewTM Red Anti-Flag Affinity Gel (Sigma) on a rotator at 4°C. The beads were washed five times using the lysis buffer, eluted using the loading buffer, and then heated for 10 min prior to being subjected to the immunoblotting analysis.

Immunoblotting assays

RAW264.7/THP-1/BMDM/hMDM cells were infected with *Ms::WT, Ms::SapM, H37Rv, H37RvΔSapM,* and *H37RvΔSapM::SapM* (MOI=10) with or without 3-Methyladenine (3-MA), Bafilomycin A1 (Baf) or Chloroquine (CQ) for 4 h. RAW_WT cells and RAW_SapM cells were then stimulated using Rapamycin with or without 3-MA, Baf, or CQ for 4h. The cells were harvested and lysed using the lysis buffer for 30 min on ice. Equal amounts of each of the proteins in every sample were separated using SDS-PAGE and electroblotted onto PVDF membranes previously blocked with 5% dry milk for 2h. The membranes with the proteins were then incubated overnight with the relevant primary antibody at 4°C and then with the relevant secondary antibody at room temperature for 1 h. The primary antibodies used were anti-mTOR, anti-Phospho-mTOR (Ser2448) , anti-Phospho-p70S6K (Thr389), anti-p70S6K, anti-Flag-Tag (Sigma), anti-β-ACTB, anti-GAPDH, anti-β-tubulin, anti-RagA, anti-RagC, anti-Rheb, anti-Phospho-Raptor (Ser792), anti-Raptor, anti-LC3, anti-Beclin1, anti-Phospho-ULK1 (Ser757), and anti-ULK1. The protein bands were visualized using ECL (NCM Biotech) according to the manufacturer's instructions and quantified using β-tubulin or β-Actin as the internal control.

Intracellular survival

RAW264.7 cells or THP-1 cells were infected with *Ms::WT*, *Ms::SapM* or *H37Rv, H37RvΔSapM,* and *H37RvΔSapM::SapM* for 12h, and the RAW_WT and RAW_SapM cells were infected with *M.smegmatis*, *H37Rv*, and *H37RvΔSapM* for 12h at MOI=10. The spent culture medium

of the infected cells was then replenished with fresh DMEM containing 200 μg/mL of amikacin and 1% antibiotic/antimycotic solution (Gibco) to kill the extracellular bacteria. Afterward, at different times, the infected macrophages were washed three times with PBS and then lysed with 1 mL of sterile water containing 0.05% Triton X-100 to release the intracellular *mycobacteria*. Subsequently, the CFU assay was performed by inoculating 50 μL of each lysate sample to the Middlebrook 7H10 agar plates followed by culture at 37°C for 3 weeks.

QUANTIFICATION AND STATISTICAL ANALYSIS

The result data were presented as mean ±SD and analyzed statistically using the GraphPad Prism software. The statistical analysis was conducted using T-test in comparison with two groups, one-way ANOVA in comparison with three groups, with $p > 0.05$ indicating non-significance (ns), *$p < 0.05$, **$p < 0.01$, ***$p < 0.001$, and **** $p < 0.0001$ as the thresholds of significance.